Optical transitions between sheets of the adiabatic potential for the Jahn-Teller system ZnSe:Cr; vibronic interactions and local lattice dynamics

A. I. Belogorokhov, M. I. Kulakov, V. A. Kremerman, A. L. Natadze, Yu. B. Rozenfel'd, and A. I. Ryskin

Institute of Semiconductor Physics, Academy of Sciences of the Lithuanian SSR

(Submitted 7 October, 1987)
Zh. Eksp. Teor. Fiz. **94**, 174–185 (June 1988)

The study of vibronic transitions within a single degenerate electronic state of the system ZnSe:Cr, i.e., transitions between the various sheets of its adiabatic potential, allows us not only to draw definite conclusions about the role of quadratic terms in the vibronic interactions (VI), but also to estimate the absolute values of the linear and quadratic IV constants. In this article we first direct our attention to the role of non-fully-symmetric VI terms in the formation of the vibrational spectrum of an impure crystal; we then show that taking these terms into account leads to a nontrivial renormalization of the vibronic spectrum. We note that the presence of even a relatively weak quadratic VI of the type under discussion can significantly renormalize the linear VI. We establish the connection between the local dynamics of the system under discussion and the character of its VI, and discuss experiments which could refine the choice of the parameters which characterize the VI.

As a rule, the local dynamics of crystal lattices with defects and the vibronic interactions (VI) in these crystals are investigated independently, although there are a number of effects which demonstrate that these effects interact strongly. The change in phonon density due to changes in masses and coupling constants has a significant effect on the strength of the vibronic coupling. On the other hand, quadratic terms in the VI determine the change in the coupling constant strength and thereby affect the local lattice dynamics.

Up to the present time, investigations of local dynamics which involve nuclear motions which are not fully symmetric relative to the defects have taken into account only fully-symmetric combinations of the quadratic VI terms. However, as we show below, the partly-symmetric combinations of these terms also have a significant effect on the local dynamics with regard to the static Jahn-Teller effect (JTE). In this work, we draw conclusions about the role of quadratic terms in the VI of the ZnSe:Cr system, which exhibits a static (tetragonal) JTE in the $^5T_2$ ground state of the tetrahedrally-coordinated Cr^+ ion (Refs. 1, 2), form an analysis of the optical transitions between equivalent minima of the adiabatic potential; in addition, we study the influence of these terms on the local dynamics of the crystal and on the strength of its vibronic coupling.

As a result of interaction of the Cr^+ ion in its $^5T_2$ state with the tetragonal e-vibration, the tetrahedron of ligands of this ion is compressed along one of the rotation-reflection fourfold axes, lowering the symmetry of the center from T_d to D_{2d} (the static JTE). When the VI are treated in linear approximation, the adiabatic potential of the vibronic single-mode T-e problem in the space of symmetrized shifts Q_θ, Q_ε of the atoms in the immediate vicinity of the Cr ion has the form of three intersecting paraboloids with minima at the points:

$$(Q_\theta=\alpha\omega_0^{-1/2}, Q_\varepsilon=0), \quad (Q_\theta=-\alpha\omega_0^{-1/2}/2, Q_\varepsilon=3^{1/2}\alpha\omega_0^{-1/2}/2),$$
$$(Q_\theta=-\alpha\omega_0^{-1/2}/2, Q_\varepsilon=-3^{1/2}\alpha\omega_0^{-1/2}/2),$$

where α is the vibronic coupling constant with the e-vibration, and ω_0 is the oscillator frequency; see Fig. 1(a). In Fig. 1(b) we show a cross section of the surfaces of the adiabatic potential in the plane $Q_\varepsilon = 0$; the symmetries of the two sheets of the potential in the group D_{2d} of the tetragonally distorted center are $^5B_2$ and ^5E. Transitions between the lower and upper sheets form a wide infrared absorption band, which was first observed in ZnSe:Cr crystals[3] and was interpreted in terms of a linear harmonic-oscillator model. In Ref. 3, certain parameters of this center (the Jahn-Teller energy and the oscillator frequency ω_0) were determined by comparing the first and second moments of the shape function of the experimental spectrum with calculated values. This determination was incorrect, since the method of moments in its tranditional form turns out to be inapplicable to situations where the spectrum, as is the case here, starts at zero frequency. It is well-known that moments of the spectral distribution are determined by differentiating a generating function with respect to time and evaluating the derivative at $t = 0$; this method does not require any knowledge of the spectral curve. If, however, the shape function is only determined for positive frequencies, then calculating the moments is just as difficult as calculating the spectral distribution. Furthermore, the authors of Ref. 3 did not include contributions from stimulated emission, which are relevant in the low-frequency region of the spectrum. A single-mode model was also used in Ref. 4 for analyzing the low-temperature infrared absorption spectra in the crystals ZnS:Cr, ZnSe:Cr, ZnTe:Cr, and CdTe:Cr.

We also note that although the single-mode model used in Refs. 3, 4 does make it possible (with the proviso that our earlier remarks are taken into account) to determine the shape of the absorption band under investigation and its temperature evolution, it also eliminates any possibility of relating the information obtained from such an investigation to the local dynamics of the system under study. This relation can be established only by carrying out an investigation of the Jahn-Teller problem which includes the real vibration spectrum of the system. We present such an investigation in what follows.

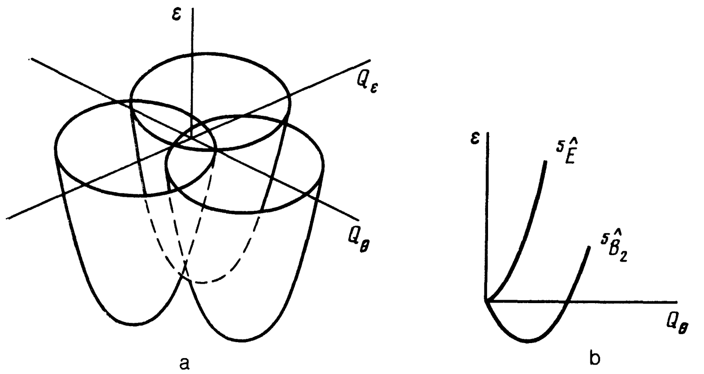

FIG. 1. (a) Adiabatic potential for the single-mode T-e problem, and (b) the cross-section of its surface in the plane $Q_\varepsilon = 0$.

EXPERIMENTAL RESULTS AND DISCUSSION

We investigated a crystal of ZnSe:Cr with a chromium content of $4.3\cdot 10^{19}$ cm^{-3}, grown from melt under an argon overpressure. The activator was introduced into the original material during growth in the form of the compound Cr_2S_3.

The transmission spectra of the sample under investigation in the region of wave numbers $\tilde{\nu} \simeq 500$–5000 cm^{-1} were recorded on a Fourier spectrometer; the transmittivity was then converted into an optical density, using a computer which was built into the apparatus. The temperature dependence of the transmission coefficient in the temperature interval $T = 8$–400 K was measured using a helium cryostat. In order to improve the signal to noise ratio, we carried out measurements of 100 spectra.

As an example, we show in Fig. 2 the absorption band connected with transitions between sheets of the adiabatic potential associated with the term $^5T_2$ for $T = 77$ K and 293 K. The intense absorption for $\tilde{\nu} < 500$ cm^{-1} is caused by second-order lattice absorption. The spectra for temperatures below room temperature are due to fine sheets (apparently several atomic layers thick) of ice in the surface of the sample. In order to identify the bands which are ice-related, we replaced the sample with the material KRS-5, which is transparent in the spectral region under study. We first obtained the transmission spectrum for a sample after lengthy pumping on the vacuum. We then lowered the vacuum in the cryostat even further and recorded the transmission spectrum under these conditions. The ratio of these spectra gives information about the absorption bands of ice.

In addition to the wide structureless band at $\tilde{\nu} \approx 500$–3000 cm^{-1} in the absorption spectrum of the system under study we observed a narrow line at $\tilde{\nu} = 598$ cm^{-1} (for $T = 8$ K), which is the first overtone of the local vibration of impurity S atoms in the crystal ZnSe. The characteristic feature of the band is the dependence of its shape on temperature, including the position of its maximum (Fig. 3) and its asymmetry.

It is well-known that the VI which are linear in the tetragonal modes cannot give rise to the experimentally-observed temperature-dependent shift in the maximum of the shape function of the band.[5] For the explanation of this shift in the band maximum, it is necessary to invoke one of the following interactions: linear VI with the trigonal t_2 modes, which, depending on the interaction strength, can give rise to the dynamic JTE; the spin-orbit interaction, which also is nondiagonal relative to the tetragonal basis and likewise can change the character of the JTE; VI which are quadratic in the e-modes; and the higher-order VI (quadratic-trigonal and cubic-tetragonal).

Interactions with the trigonal t_2 modes are dynamic, and as a result are suppressed by the linear static interactions with the e-modes.[6,7] This suppression is analogous to the

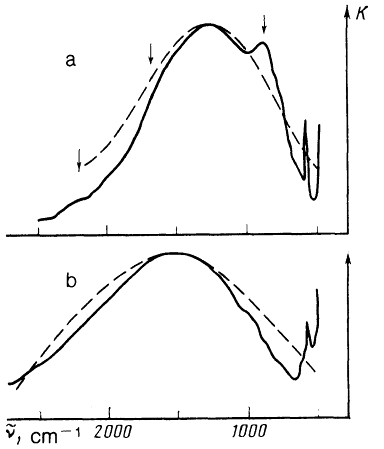

FIG. 2. Experimental (solid line) and calculated (dashed line) spectral dependence of the IR absorption coefficient $K(\tilde{\nu})$ for (a) 77 K; (b) 295 K. The arrows show the most intense lines of the ice absorption.

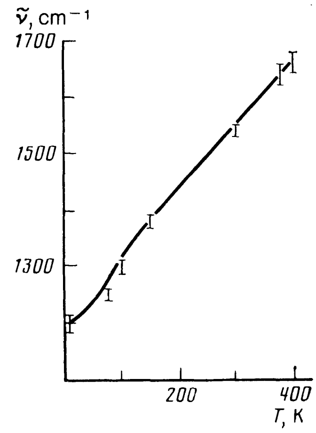

FIG. 3. Experimental (vertical segments) and theoretical (solid line) values of the position of the IR absorption maximum as a function of temperature.

Ham factors which are introduced in the first- and second-order vibronic reduction of electronic quantities.[8] Since the interactions with the t-modes are suppressed by linear interactions with the e-modes, they must be effectively weak. Thus, in our situation we must first of all take into account the quadratic interactions with e-modes and only then the dynamic VI as necessary.

The second of the mechanisms listed above also can be discarded, because the spin-orbit interaction constant equals zero in the $^5T_2$ ground state of the Cr^{2+} ion.[2]

As we show in this work, the temperature evolution of the absorption band connected with transitions within the T-term are satisfactorily explained by taking into account quadratic vibronic interactions with the e-modes.

THE SHAPE FUNCTION OF THE SPECTRAL CURVE

The optical absorption coefficient $K(\omega)$ has the following form, to within constant factors:

$$K(\omega)=(1-e^{-\omega/kT})f(\omega)\,\omega. \tag{1}$$

Here and below we will set $\hbar = 1$. The shape function for the transition has the form

$$f(\omega)=\theta(\omega)\int_{-\infty}^{\infty} dt\, e^{-i\omega t}\langle d^+d(t)\rangle. \tag{2}$$

Here, d is the dipole moment operator, while $d(t)$ is the d-operator in the Heisenberg representation: $d(t) = \exp(iHt)\, d \exp(-iHt)$; the angular brackets denote statistical averaging. Our definition of the shape function differs from the usual one[5] since we have separated out the factor $\theta(\omega)$.

The Hamiltonian H for this impurity-phonon system, including the relevant VI terms, has the form

$$H=H_0+V_e+V_{e^2},\qquad H_0=\frac{1}{2}\sum_\chi (p_\chi^2+\omega_\chi^2q_\chi^2)C_{A1},$$

$$V_e=\omega_e^{3/2}\alpha\sum_\chi q_\chi[C_{E\theta}a_\chi(E\theta)+C_{E\varepsilon}a_\chi(E\varepsilon)],$$

$$V_{e^2}=\omega_e^2C_{A1}c\sum_{\chi\chi'} q_\chi q_{\chi'}[a_\chi(E\theta)a_{\chi'}(E\theta)+a_\chi(E\varepsilon)a_{\chi'}(E\varepsilon)]$$

$$+\,\omega_e^2W\sum_{\chi\chi'} q_\chi q_{\chi'}\{C_{E\theta}[a_\chi(E\varepsilon)a_{\chi'}(E\varepsilon)-a_\chi(E\theta)a_{\chi'}(E\theta)]$$

$$+2C_{E\varepsilon}a_\chi(E\theta)a_{\chi'}(E\varepsilon)\}, \tag{3}$$

where H_0 is the phonon Hamiltonian, q_χ and p_χ are the coordinate and momentum of the χth vibration, $a_\chi(E\gamma)$ ($\gamma = \theta,\varepsilon$) are the Van Vleck coefficients, $C_{E\gamma}$ is a matrix of electronic operators which transform according to the γth row of the irreducible representation E in the basis of unperturbed functions of the T-term[5] (C_{A1} is the unit matrix),

$$\omega_e=\left[\sum_\chi \frac{a_\chi^2(E_\gamma)}{\omega_\chi^2}\right]^{-1/2},$$

V_e is the VI operator which is linear in the e-modes, α is the dimensionless constant for this interaction. The VI operator V_{e^2}, which is quadratic in the e-mode, consists of two terms, one of which contains the fully symmetric combination of symmetrized nuclear displacements, while the second contains the partly symmetric combinations which transform according to the θ and ε rows of the E representation (the symmetrized square $\{E^2\} = A_1 + E$). The corresponding dimensionless vibronic coupling constants are denoted by c (for the fully symmetric combination) and W(for the partly symmetric combination).

The linear interaction with the e-modes for the ground state of the Cr^{2+} is quite strong,1) and leads to the static JTE. If we limit ourselves to including only this interaction, the derivative of the optical transition function $\langle d^+d(t)\rangle$ can be calculated exactly with the help of standard methods of multiphonon processes[5]; the resulting $f(\omega)$ has the Pekar form, whose maximum, as is well-known, does not shift with a change in temperature. The exponential term in the absorption coefficient (1), which describes the induced processes, causes a high-frequency shift in the maximum with increasing temperature, which is also observed in experiment. However, since the frequency of the maximum satisfies $\omega_m \sim 10^3$ cm^{-1}, this shift mechanism cannot play a significant role in the temperature range under investigation. Thus, linear VI with the static tetragonal modes cannot explain the experimentally observed dependence of the absorption coefficient curve. An exact calculation of $f(\omega)$, taking into account the VI with the leading terms for the interaction with the static modes, is impossible; therefore we will use an approximate method, which we describe in what follows.

Let us introduce the quantities Ω_n, equal to

$$\Omega_n=(-i)^n\frac{d^n\langle d^+d(t)\rangle}{dt^n}\bigg|_{t=0}. \tag{4}$$

We will call these quantities "moments," although the Ω_n are actually moments not of the real spectral distribution $f(\omega)$, but rather of a distribution in which $f(\omega)$ formally is continued into the region of negative frequencies. Knowledge of these moments allows us to recover the form of the desired distribution by using the well-known Edgeworth series[9]; this distribution coincides with $f(\omega)$ in the region of positive frequencies. We will use the first three terms of the Edgeworth series.

Let us note once more: the moments computed using Eq. (4) must not be directly compared with the experimental moments of the curve $K(\omega)/\omega$, as was done in Ref. 3.

QUADRATIC VI WITH THE TETRAGONAL MODES

We investigate the way the quadratic VI with the e-mode affects the spectrum. By virtue of the statistical character of the interaction, the problem of describing the form of the IR absorption under study is analogous to the problem of calculating singlet-singlet optical transitions which are accompanied by variation of the equilibrium positions of the nuclei and by the "frequency effect".[10] By the "frequency effect" we mean phenomena connected both with the difference between frequencies of the normal oscillations in the initial and final states, and with the absence of a general system of normal coordinates for these states. In Ref. 10, general expressions were introduced for the generating functions and for the moments. However, computations of the generating functions using Eq. (3.11) of Ref. 10, taking into account the phonon dispersion, cannot be carried through to numerical values, even when the frequency effect possesses a local character, i.e., when the problem of finding the redefined spectrum is exactly soluble. In connection with this we will use the method with the modification proposed above for describing the shape-function: for $\omega > 0$,

$$f(\omega)=\frac{1}{N}\left[\varphi(x)-\frac{\gamma_1}{6}\varphi^{(3)}(x)+\frac{\gamma_2}{24}\varphi^{(4)}(x)\right], \tag{5}$$

where N is a normalization factor, $x=(\omega-\Omega_1)\sigma_2^{-1/2}$, $\varphi(x)=\exp(-x^2/2)$,

$$\gamma_1=\sigma_3\sigma_2^{-3/2}, \qquad \gamma_2=(\sigma_4-3\sigma_2^2)\sigma_2^{-2}, \tag{6}$$

and σ_n is the nth centered moment of the distribution which corresponds to continuing $f(\omega)$ (see Eq. 2) formally into the region of negative frequencies.

Let us calculate the moments entering into (5), (6). For this we introduce the retarded phonon Green's functions for the initial and final states of the transition, corresponding to the electronic states $|T_2\zeta)$ and $|T_2\xi)$ (by virtue of the symmetry of the problem, it is sufficient to calculate the contribution to $K(\omega)$ of the transition between these states):

$$\hat{G}_\zeta=(z^2\sigma_0-\hat{\Omega}_3^2+i\delta)^{-1}, \qquad \hat{G}_\xi=(z^2\sigma_0-\hat{\Omega}_\xi^2+i\delta)^{-1}. \tag{7}$$

Here, σ_0 is the two-dimensional unit matrix, and Ω_ζ^2 and Ω_ξ^2 are the dynamic matrices for the system in the electronic states $|T_2\zeta)$ and $|T_2\xi)$:

$$\hat{\Omega}_\zeta^2=\hat{\omega}^2+w\hat{A}+\varepsilon B, \qquad \hat{\Omega}_\xi^2=\hat{\omega}^2-w\frac{\hat{A}}{2}-w\frac{\sqrt{3}}{2}\hat{a}+\varepsilon\hat{B},$$

$$w=2\omega_e^2W, \qquad \varepsilon=2\omega_e^2c, \qquad \omega_{\chi\chi'}^{2}=\omega_\chi^2\delta_{\chi\chi'}\sigma_0. \tag{8}$$

The matrices $\hat{A}$, $\hat{a}$, and $\hat{B}$ are given by

$$\hat{A}=\begin{pmatrix}\mathbf{a}(E\theta)\otimes\mathbf{a}(E\theta) & 0\\ 0 & -\mathbf{a}(E\varepsilon)\otimes\mathbf{a}(E\varepsilon)\end{pmatrix},$$

$$\hat{a}=\begin{pmatrix}0 & \mathbf{a}(E\theta)\otimes\mathbf{a}(E\varepsilon)\\ \mathbf{a}(E\varepsilon)\otimes\mathbf{a}(E\theta) & 0\end{pmatrix},$$

$$\hat{B}=\begin{pmatrix}\mathbf{a}(E\theta)\otimes\mathbf{a}(E\theta) & 0\\ 0 & \mathbf{a}(E\varepsilon)\otimes\mathbf{a}(E\varepsilon)\end{pmatrix}. \tag{9}$$

Here $\mathbf{a}(E\gamma)\otimes\mathbf{a}(E\gamma')$ denotes the direct product of the Van Vleck vector coefficients. The poles of $\hat{G}_\zeta$ and $\hat{G}_\xi$ give the phonon spectrum renormalized by the quadratic interaction, while their imaginary parts are proportional to the renormalized phonon densities of states.

According to Ref. 10, the first moment Ω_1 equals

$$\Omega_1={}^1/_2(\mathbf{X}_\zeta-\mathbf{X}_\xi)\hat{\Omega}_\xi^2(\mathbf{X}_\zeta-\mathbf{X}_\xi)$$
$$+{}^1/_4\,\mathrm{Sp}\,[\hat{\Omega}_\zeta^{-1}\,\mathrm{cth}\,(\beta\hat{\Omega}_\zeta/2)\,(\hat{\Omega}_\xi^2-\hat{\Omega}_\zeta^2)], \tag{10}$$

where $\mathbf{X}_\zeta$, $\mathbf{X}_\xi$ are the coordinates of the minima of the adiabatic potentials in the states $|T_2\zeta)$ and $|T_2\xi)$ over the sets $a_\chi(E\theta)q_\chi$, $a_\chi(E\varepsilon)q_\chi$:

$$\mathbf{X}_\zeta=\alpha\omega_e^{3/2}\hat{\Omega}_\zeta^{-2}\begin{pmatrix}\mathbf{a}\ (E\theta)\\ 0\end{pmatrix}, \qquad \mathbf{X}_\xi=-\alpha\omega_e^{3/2}\hat{\Omega}_\xi^{-2}\begin{pmatrix}\mathbf{a}(E\theta)/2\\ -\sqrt{3}\mathbf{a}(E\varepsilon)/2\end{pmatrix}. \tag{11}$$

Substituting (11) and the expression for Ω_ξ^2 from (8) into (10), we find

$$^1/_2(\mathbf{X}_\zeta-\mathbf{X}_\xi)\hat{\Omega}_\xi^2(\mathbf{X}_\zeta-\mathbf{X}_\xi)=3\omega_e\alpha^2(1+2c+W)/2(1+2c+2W)^2. \tag{12}$$

Let us express $\hat{\Omega}_\zeta^{-1}\mathrm{cth}(\beta\hat{\Omega}_\zeta/2)$ through the imaginary part of $\hat{G}_\zeta$:

$$\hat{\Omega}_\zeta^{-1}\,\mathrm{cth}\,\frac{\beta\hat{\Omega}_3}{2}=\int_0^\infty dz\,\delta(z-\hat{\Omega}_\zeta)\frac{1}{z}\,\mathrm{cth}\,\frac{\beta z}{2}$$
$$=-\frac{1}{\pi}\int_0^\infty dx\,\frac{\mathrm{Im}\,\hat{G}_\zeta(x)}{x^{1/2}}\,\mathrm{cth}\,\frac{\beta x^{1/2}}{2}.$$

Introducing the renormalized density of states $\rho(x)$, which equals

$$\hat{\rho}(x)=-\pi^{-1}\,\mathrm{Im}\,\hat{G}_\zeta(x),$$

we obtain

$$\hat{\Omega}_\zeta^{-1}\,\mathrm{cth}\,\frac{\beta\hat{\Omega}_\zeta}{2}=\int_0^\infty dx\,\frac{\hat{\rho}(x)}{x^{1/2}}\,\mathrm{cth}\,\frac{\beta x^{1/2}}{2}. \tag{13}$$

Substituting (13), (8) and (12) into expression (10) for Ω_1, we find that

$$\Omega_1=\frac{3\omega_e\alpha^2(1+2c+W)}{2(1+2c+2W)^2}$$
$$-\frac{w}{4}\int_0^\infty\frac{dx}{x^{1/2}}\,\mathrm{cth}\,\frac{\beta x^{1/2}}{2}\,\mathrm{Sp}\,\hat{\rho}(x)\left(\frac{3}{2}\hat{A}+\frac{\sqrt{3}}{2}\hat{a}\right), \tag{14}$$

i.e., Ω_1 is expressed through the imaginary part of $\hat{G}_\zeta$. We can also express the higher moments using $\hat{G}_\zeta$, $\hat{G}_\xi$. Thus, the problem of computing the moments reduces to a calculation of $\hat{G}_\zeta$, $\hat{G}_\xi$. These Green's functions can be calculated exactly as a consequence of the local character of the quadratic VI. The latter is manifested explicitly in the configuration space of nuclear displacements and leads to the fact that the system of equations for the Green's function is finite in size.

In wave-vector space the local character is manifest in the fact that the matrices $\hat{A}$, $\hat{a}$, and $\hat{B}$, which enter into the dynamic matrices $\hat{\Omega}_{\zeta^2}$ $\hat{\Omega}_{\xi^2}$, possess the properties of projections

$$\hat{a}\hat{G}_0\hat{a}=\hat{A}\hat{G}_0\hat{A}=D_0\hat{B}, \qquad \hat{A}\hat{G}_0\hat{a}=D_0\sigma_z\hat{a}, \tag{15}$$

where

$$\hat{G}_0=\frac{1}{z^2\sigma_0-\hat{\omega}^2+i\delta}, \qquad D_0=\sum_\chi\frac{a_\chi^2(E\theta)}{z^2-\omega_\chi^2+i\delta}.$$

The above properties allow us to calculate $\hat{G}_\zeta$ and $\hat{G}_\xi$. Omitting the transformation, we present the final expressions:

$$\hat{G}_\zeta=\hat{G}_0+\{w\hat{G}_0\hat{A}\hat{G}_0+[\varepsilon+(w^2-\varepsilon^2)D_0]\hat{G}_0\hat{B}\hat{G}_0\}$$
$$\times\ [(1-\varepsilon D_0)^2-w^2D_0^2]^{-1},$$
$$\hat{G}_\xi=\hat{G}_0-\{{}^1/_2w\hat{G}_0\hat{A}\hat{G}_0-(\sqrt{3}/2)w\hat{G}_0\hat{a}\hat{G}_0$$
$$-[\varepsilon+(w^2-\varepsilon^2)D_0]\hat{G}_0\hat{B}\hat{G}_0\}[(1-\varepsilon D_0)^2-w^2D_0^2]^{-1}. \tag{16}$$

In the electronic state $|T_2\zeta\rangle$, the modes which transform according to the θ- and ε-rows of the E-representation are orthogonal to each other, which allows us to introduce the symmetrized Green's functions:

$$D_\theta=(\mathbf{a}(E\theta);0)\hat{G}_\zeta\begin{pmatrix}\mathbf{a}(E\theta)\\ 0\end{pmatrix}=\frac{D_0}{1-D_0(w+\varepsilon)},$$

$$D_\varepsilon=(0;\mathbf{a}(E\varepsilon))\hat{G}_\zeta\begin{pmatrix}0\\ \mathbf{a}(E\varepsilon)\end{pmatrix}=\frac{D_0}{1-D_0(\varepsilon-w)}. \qquad (17)$$

Introducing the normalized projected density of states

$$\rho_\gamma=-\pi^{-1}\,\mathrm{Im}\,D_\gamma(z) \qquad (18)$$

($\gamma=\theta,\varepsilon$), we obtain the final expression for Ω_1:

$$\Omega_1={}^3/_2\omega_e\alpha^2(1+2c+W)/(1+2c+2W)^2+{}^3/_4\omega_e^2W(S_\varepsilon-S_\theta), \qquad (19)$$

where

$$S_\gamma=\int_0^\infty dx\,x^{-1/2}\rho_\gamma(x)\,\mathrm{cth}\frac{\beta x^{1/2}}{2}.$$

Analogously, we calculate all the higher moments. We also have obtained an expression for the fourth moment, which was not given in Ref. 10. In view of its cumbersomeness, we present only the final expressions for σ_2, σ_3 and $\sigma_4-3\sigma_2^2$, retaining only terms which are proportional to the square of the e-mode linear coupling constant α; because the inequalities $c, W\ll\alpha$ hold in our case [in (19) terms proportional to W are retained, since the entire effect of the temperature dependence of Ω_1 is due only to these terms]:

$$\sigma_2={}^3/_8\alpha^2\omega_e^3[3S_\theta(1+2c)^2+S_\varepsilon(1+2c+4W)^2]/(1+2c+2W)^2, \qquad (20)$$

$$\begin{aligned}\sigma_3={}&{}^3/_2\alpha^2\omega_e^3[1-2W(1+2c)/(1+2c+2W)^2]\\&-{}^{27}/_8w\alpha^2\omega_e^3[{}^3/_4S_\theta^2-{}^1/_2S_\theta S_\varepsilon-{}^1/_4S_\varepsilon^2-W(3S_\theta S_\varepsilon\\&+S_\varepsilon^2)/(1+2c+2W)+W^2(3S_\theta^2+2S_\theta S_\varepsilon-S_\varepsilon^2)/\\&(1+2c+2W)^2],\end{aligned} \qquad (21)$$

$$\begin{aligned}\sigma_4-3\sigma_2^2={}&{}^3/_2\alpha^2\omega_e^3\{{}^3/_4I_\theta+{}^1/_4I_\varepsilon+6\omega_e^2W(S_\varepsilon-S_\theta)\\&+W[I_\varepsilon-3I_\theta+12\omega_e^2W(3S_\theta+S_\varepsilon)]/(1+2c+2W)\\&+W^2[3I_\theta+I_\varepsilon-48\omega_e^2WS_\theta]/(1+2c+2W)^2\}\\&+{}^{27}/_4\alpha^2\omega_e^7W^2[{}^1/_2(9S_\theta^3-3S_\theta^2S_\varepsilon+7S_\theta S_\varepsilon^2+3S_\varepsilon^3)\\&-2W(9S_\theta^3+3S_\theta^2S_\varepsilon-S_\theta S_\varepsilon^2-3S_\varepsilon^3)/(1+2c+2W)\\&+2W^2(9S_\theta^3+9S_\theta^2S_\varepsilon-5S_\theta S_\varepsilon^2+3S_\varepsilon^3)/(1+2c+2W)^2].\end{aligned} \qquad (22)$$

Here,

$$I_\gamma=\int_0^\infty dx\,x^{1/2}\rho_\gamma(x)\,\mathrm{cth}\frac{\beta x^{1/2}}{2}.$$

In order to calculate the renormalized phonon density of states which enters into Eqs. (19)–(22), we calculate the bare projected density of e-vibrations (relative to the cation position) for the crystal ZnSe; the calculation is carried out using a ten-parameter shell model of the lattice dynamics.[11]

The parameters for the linear and quadratic VI (α, c and W) were determined by the method of least squares, based on the best agreement between the calculated and experimental temperature shifts in the maximum of the spectral curve for the absorption coefficient. It was found that two significantly different choices of these parameters correspond to the minimum mean-square deviation:

$$\alpha_1^2=14.5,\quad c_1=0,\quad W_1=0.35, \qquad (23)$$

$$\alpha_2^2=0.9,\quad c_2=0.025,\quad W_2=-0.375. \qquad (24)$$

In Fig. 3, we show the calculated curve for the temperature shift of the maximum in the absorption band for the choice of parameters (23): the curve for choice (24) differs from it only very slightly. The agreement between the experimentally and theoretically determined shifts can be considered good. We may also consider the agreement between the experimental and theoretical spectral curves (Fig. 2) fully satisfactory, especially if we take into account the fact that the method we are using to calculate the shape of the spectral curve (the Gram-Charles-Edgeworth series) is significantly less accurate on the wings of the curve than it is near the maximum.

THE EFFECT OF LOCAL LATTICE DYNAMICS ON SPECTRAL PHENOMENA ASSOCIATED WITH THE JTE

Let us investigate the influence of the quadratic VI on the local dynamics of the system under study, and discuss the physical nature of the two situations (23) and (24), both of which describe the IR absorption spectrum equally well.

In Fig. 4 we denote by a the bare projected density of tetragonal vibrations in the crystal ZnSe, i.e., the vibrations

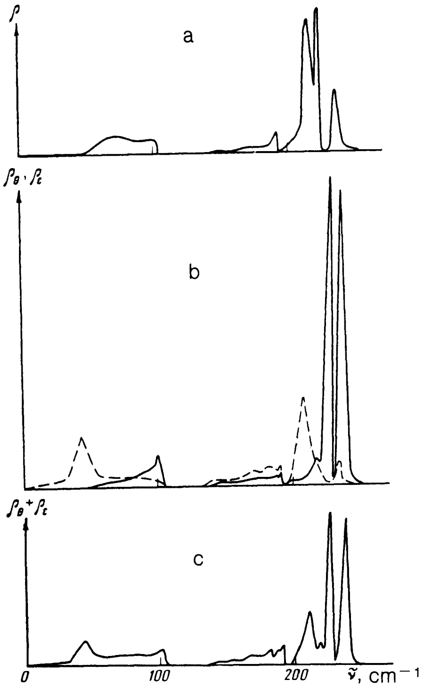

FIG. 4. (a) Projected density of the e-vibrations of the anion in the ZnSe crystal; (b) Renormalized densities of the θ and ε components of the ligand displacements of the impurity Cr^{2+} ion (the solid and dashed lines, respectively); (c) Total density of tetragonal vibrations in the ZnSe:Cr crystal.

which possess e-symmetry relative to the cation position; by b the renormalized densities for the θ and ε components of the symmetrized displacements of the ligands around the Cr^+ ion for the choice (23); by c the total density of tetragonal vibrations $\rho_\theta + \rho_\varepsilon$. The change in the spectral density of the θ and ε components is determined by the signs of the corresponding combinations of strength constants $c + W$ and $c - W$. A positive sign of these combinations leads to an increase in the strength constant and to a displacement of the corresponding density in the high-frequency region up to the appearance of local vibrations. The negative sign of $c \pm W$ redistributes the densities ρ_θ and ρ_ε in the low-frequency region, which can result in the appearance of low-frequency quasilocalized modes. For such values of the parameters c and W, when one of the combinations is positive while the second is negative, the total density can have a very unusual form. In particular, by using the choice (23) for this system, we simultaneously see both a low-frequency ($\tilde{\nu} \approx 45$ cm^{-1}) and a high-frequency ($\tilde{\nu} \approx 240$ cm^{-1}) quasilocal mode in the vibrational spectrum—a situation which is excluded when only the fully symmetric terms of the quadratic VI are included.

Since $c_1 = 0$, $c_2 \approx 0$, and $W_1 \approx - W_2$, in going from choice (23) to choice (24) ρ_θ and ρ_ε practically change places, so that the total density of tetragonal vibrations remain almost unchanged. Therefore, for the present system the vibrational spectrum in each of three equivalent minima of the adiabatic potential does not depend on the sign of W. However, this sign determines the shape of its adiabatic potential. The qualitative dependence of this shape on the sign of W can be investigated within the framework of a single-mode model, once we replace the real spectrum of the e-vibrations of a perfect crystal by one two-dimensional oscillator with frequency ω_0, which, interacting with the Cr^+ ion in the $^5T_2$ state, is split into one-dimensional oscillators with frequencies ω_θ and ω_ε which are renormalized by the quadratic VI:

$$\omega_\theta^2=\omega_0^2(1+2W), \quad \omega_\varepsilon^2=\omega_0^2(1-2W).$$

The coordinates of the adiabatic potential minimum along the Q_θ axis are

$$Q_\theta^0 \sim \alpha/\omega_\theta^2=\alpha/\omega_0^2(1+2W), \quad Q_\varepsilon^0=0. \tag{25}$$

In Fig. 5 we present the cross-section of the adiabatic potential for this single-coordinate model in the plane parallel to Q_θ, Q_ε, for zero, positive and negative values of the parameter W. For $W \neq 0$, the circular paraboloids turn into elliptic paraboloids; Fig. 5 shows the dependence of the equilibrium positions and orientations of these elliptic paraboloids on the sign of W when we include the incompletely symmetric quadratic VI terms. It is clear from Eq. (25) that for $W < 0$ the effective frequency ω_θ decreases while the vibronic coupling with the θ-mode is amplified; these effects result in a large shift in the equilibrium position. Physically, this result is understandable: the smaller the oscillator frequency, the larger the equilibrium position shift that results from a given coupling. The opposite situation arises for $W > 0$.

It is natural to choose the heat release as a parameter which characterizes the magnitude of the vibronic coupling. We measure this quantity using the square of the effective vibronic coupling constant:

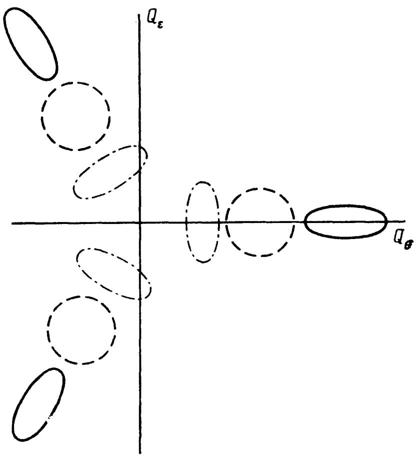

FIG. 5. Cross section of the adiabatic potential for the single-mode T-e problem, taking into account the quadratic incompletely symmetric VI, in the plane parallel to Q_θ, Q_ε; the dashed lines are for $W = 0$, the solid lines for $W < 0$ and the dotted-dashed lines are for $W > 0$.

$$\alpha_{eff}^2=E_{JT}/\hbar\omega_\theta \sim \alpha^2/\omega_\theta^3 \sim \alpha^2/(1+2W)^{3/2}. \tag{26}$$

This parameter has practically the same value $\alpha_{\text{eff}}{}^2 \approx 6$ for the two choices of parameters (23) and (24); at the same time, the physical situations corresponding to these choices are quite different. In the first case, i.e., (23), the very strong bare linear static (tetragonal) JTE is considerably weakened due to the increase in the effective frequency which determines the positions of the adiabatic potential minima—see Fig. 5. In the second case, i.e., (24), there occurs a still more significant amplification of the vibronic coupling, which transforms the static JTE with intermediate coupling $\alpha^2 = 0.9$ into strong coupling.

Analysis of Eqs. (19)–(22) shows that the following three combinations of parameters for the linear and quadratic vibronic couplings enter into these expressions, which determine the shape of the spectral curve for the intersheet transition: $\alpha^2 W/(1 + 2W)^2$, $\alpha^2/(1 + 2W)$ and $W^2(1 - 4W^2)$; out of these three, the first two depend on the sign of W, while the last one does not. These parameters also describe how the local dynamics of nuclei in the immediate vicinity of the center affects the magnitude of the vibronic coupling. We note that they are in no way connected with the single-coordinate model used to describe the effective coupling constant (26).

In order to choose one of the two sets (23) and (24) of vibronic constants, it is necessary to analyze thoroughly those experiments in which the projected density of states, which determine the shifts in the adiabatic potential minima, could manifest itself. One such experiment could be the measurement of the luminescence spectrum of the $E \rightarrow T_2$ transition in the ion Cr^{2+} (Ref. 12), which has a quite well-expressed vibronic spectrum in contrast to the completely structureless absorption curve connected with transitions within the $^5T_2$. In addition, experiments involving nonresonant Raman light scattering induced by impurities in the ZnSe system could turn out to be extremely relevant in this regard; such experiments can give information about the low-frequency spectrum, which in our experiments was masked by characteristic lattice absorption. Furthermore, we expect a very characteristic polarization dependence in the Raman scattering spectrum connected with the two possible symmetries T_2 and E of the tensor electronic polarization. In the first case, the Raman scattering in practice must coincide with the wide structureless band of the IR absorption under study; in the second case, it must describe the processes of single-phonon absorption within one of the minima of the adiabatic potential, i.e., must reproduce the shape of the renormalized vibrational spectrum $1/2\ (\rho_\theta + \rho_\varepsilon)$.

CONCLUSION

In summary, our investigation of the temperature evolution of the IR absorption band connected with transitions within the $^5T_2$ term has allowed us to obtain quite complete (although somewhat ambiguous) information about the quadratic VI in this system, uncomplicated by anharmonic shifts which take place for transitions between the various electronic states. In order to describe an absorption spectrum beginning from zero frequency, we have proposed a modification of the method of moments which describes the shape function formally continued into the region of negative frequencies. The moments are related to the phonon Green's functions, which can be calculated exactly as a consequence of the local interaction which corresponds to the frequency effect.

We have shown that including the incompletely symmetric combinations of the quadratic VI terms leads to a nontrivial renormalization of the vibrational spectrum of the impure crystal, in which there occurs a lifting of the degeneracy of the twofold-degenerate phonon mode along with a shift in the densities of its components; one component shifts into the high frequency, the other into the low frequency region of the spectrum.

The quadratic VI significantly redefines the linear VI; therefore, the values of the linear parameters obtained for the majority of the systems studied up to the present time

---

1) As we will verify later, this assertion needs to be made more precise, since the magnitude of the linear vibronic coupling depends in a significant way on the quadratic VI terms, which change the phonon spectrum and renormalize the linear interactions. Nevertheless, experiment shows that for the ground state of the Cr^{2+} ion in ZnSe the renormalized linear interaction with the tetragonal modes is strong.

[1] J. T. Vallin, G. A. Slack, S. Roberts and A. E. Hughes, Phys. Rev. **B2**, 4313 (1970).

[2] J. T. Vallin, G. D. Watkins, Phys. Rev. **B9**, 2051 (1974).

[3] B. Nygren and J. T. Vallin, Solid State Commun. **11**, 35 (1972).

[4] M. Kaminska, J. M. Baranowsky, S. M. Uba and J. T. Vallin, J. Phys. **C12**, 2197 (1979).

[5] Yu. E. Perlin and B. S. Tsukerblat, *Effekty Elektronno-Kolebatel'nogo Vzaimodeistviya v Opticheskykh Spektrakh Primesnnykh Paramagnitnykh Ionov* (*The Effects of Electronic-Vibronic Interaction on the Optical Spectrum of Paramagnetic Impurity Ions*). Kishinev: ShTIINTsA, 1974, ch. 2.

[6] V. Z. Polinger, Zh. Eksp. Teor. Fiz. **77**, 1503 (1979) [Sov. Phys. JETP **50**, 754 (1979)].

[7] V. A. Kremerman and Yu. B. Rozenfel'd, Lith. Phys. Coll. **26**, 162 (1986).

[8] F. S. Ham, *Electron Paramagnetic Resonance* (New York: Plenum Press, 1972), p. 1.

[9] M. Lax, *Problemy Fiziki Poluprovodnikov* (*Problems in the Theory of Semiconductors*). Moscow: IIL, 1957, p. 407.

[10] R. Kubo and Y. Toyozawa, *Fiziki Poluprovodnikov* (*Problems in the Theory of Semiconductors*). Moscow: IIL, 1957, p. 442.

[11] D. N. Talwar, M. Vandevyver, K. Kunc, and M. Zigone, Phys. Rev. **B24**, 741 (1981).

[12] G. Grebe, G. Rousson, and H.-J. Schultz, J. Luminescence **12/13**, 701 (1976).

Translated by Frank J. Crowne